



ACDIV-2013-04  
February 18<sup>th</sup>, 2013

## ALBA Top-up safety simulations

G. Benedetti

### Abstract:

The potential hazards introduced by injecting into the ALBA storage ring with front end shutters open are determined through particle tracking simulations. The method is based on the possible overlap between phase space of forwards and backwards tracking between the straight section downstream of the front end and the beamline. Realistic magnetic field, trajectory, aperture and energy errors are taken into account. Scenarios that could bring an injected beam of electrons passing through an open beamline front end are identified and the interlocks to prevent them are discussed.

Accelerator Division  
Alba Synchrotron Light Source  
Ctra. BP 1413 Km. 3,3  
08290 Cerdanyola del Valles, Spain



## ACCELERATOR DIVISION

<i>ALBA Project Document</i>	<i>EDMS Document No.</i>	<i>Created:</i> 18.02.13	<i>Page:</i> 1/17
<b>ACDIV-2013-04</b>		<i>Modi</i>	<i>Rev.</i> 0

### ALBA Top-up safety simulations

#### *Abstract*

The potential hazards introduced by injecting into the ALBA storage ring with front end shutters open are determined through particle tracking simulations. The method is based on the possible overlap between phase space of forwards and backwards tracking between the straight section downstream of the front end and the beamline. Realistic magnetic field, trajectory, aperture and energy errors are taken into account. Scenarios that could bring an injected beam of electrons passing through an open beamline front end are identified and the interlocks to prevent them are discussed.

<i>Prepared by:</i> <b>G. Benedetti</b>	<i>Checked by:</i>	<i>Approved by:</i>
<i>Authorship:</i>		

*Distribution list:*

ALBA Project Document No:	Page: 2/17
<b>ACDIV-2013-04</b>	Rev. No. 0.0

<b><i>Record of Changes</i></b>			
<i>Rev. No.</i>	<i>Date</i>	<i>Pages</i>	<i>Description of changes</i>

ALBA Project Document No:	Page: 3/17
<b>ACDIV-2013-04</b>	Rev. No. 0.0

### *References*

- [1] *L. Emery, M. Borland, "Analytical Studies of Top-Up Safety for the Advanced Photon Source", PAC99, New York, 1999.*
- [2] *M. Borland, L. Emery, "Tracking Studies of Top-Up Safety for the Advanced Photon Source", PAC99, New York, 1999.*
- [3] *H. Nishimura et al., "Beam Loss Simulation Studies for ALS Top-Off Operation", PAC05, Knoxville, 2005.*
- [4] *H. Nishimura et al., "Advanced Light Source's Approach to Ensure Conditions for Safe Top-Off", NIM-A 608, 2009.*
- [5] *X. Huang, "Tracking Study for Top-Off Safety Validation at SSRL", NIM-A 635, 2011.*
- [6] *Y. Li et al., "Efficient Cascaded Parameter Scan Approach for Studying Top-Off Safety in Storage Rings", PhysRevSTAB 14, 2011.*
- [7] *I. Martin, "Top-Up Safety Simulations for the Diamond Storage Ring", IPAC08, Genoa, 2008.*
- [8] *I. Martin, "Plans for Top-Up at Diamond", presentation at TOP-UP Workshop, Melbourne, 2009.*
- [9] *H.J. Tsai et al., "Top-Up Safety Simulations for the TPS Storage Ring", IPAC11, San Sebastián, 2011.*
- [10] *A. Terebilo, "Accelerator Modeling with Matlab Accelerator Toolbox", PAC01, Chicago, 2001.*
- [11] *Private communication with E. Al-Dmour.*
- [12] *Private communication with J. Campmany.*
- [13] *Private communication with J. Marcos.*



*Table of Contents*

1. INTRODUCTION .....	5
2. METHOD .....	5
2.1. Outline of simulation procedure .....	5
2.2. Tracking code description .....	6
2.3. Definition of particle phase spaces .....	7
2.4. Error Scenarios.....	7
2.4.1. Magnet Strength Variations .....	7
2.4.2. Aperture Misalignments .....	7
2.4.3. Energy Errors .....	7
2.5. Method Demonstration .....	8
3. ID BEAMLINES (BL04, BL11, BL13, BL22, BL24, BL29).....	9
3.1. Magnet arrangement and apertures .....	9
3.2. Injected beam energy error .....	9
3.3. Single dipole failure .....	10
3.4. Single quadrupole failure.....	11
3.5. Single sextupole failure .....	11
3.6. Worst scenario combining events .....	12
4. DIPOLE BEAMLINE (BL09).....	12
4.1. Magnet arrangement and apertures .....	12
4.2. Injected beam energy error .....	13
4.3. Single dipole failure .....	14
4.4. Single quadrupoles failure.....	14
4.5. Single sextupole failure .....	15
4.6. Worst scenario combining events .....	17
5. DISCUSSION.....	17

ALBA Project Document No:	Page: 5/17
<b>ACDIV-2013-04</b>	Rev. No. 0.0

## 1. INTRODUCTION

Before top-up operation can be offered to users at the ALBA, it must be demonstrated that personnel safety is maintained. During top-up, the main safety concern is that a mis-steered injected beam of electrons could leave the storage ring intact and exit through an open beamline shutter. If this beam were to then strike an object in the beamline, a person standing close to the optics hutch wall could potentially receive a large radiation dose. The work described in this report aims to demonstrate that an accident of this type cannot occur, even considering a wide range of realistic magnetic, trajectory or electron beam energy errors. Since the number of possible error scenarios is very large, and that only a small subset of these can be tested on the machine, a program of tracking studies has been undertaken to perform the task of identifying any situations which could lead to a top-up accident. Such studies have also been performed at other light, the conclusions of which are generally machine-specific [1-9].

The primary role of the tracking studies is to identify any error, or any particular combination of errors, which would lead to a beam of electrons passing through an open beamline shutter. Then the next task is to identify an interlock system which would prevent the situation from occurring while the beam is being injected. One interlock already implemented is the stored beam interlock, where top-up injection is inhibited if the stored beam current drops below a pre-determined threshold, as the absence of stored beam indicates a possible fault in the storage ring. This constraint is sufficient to exclude a large number of possible accident scenarios, such as a significant drop in dipole field strength.

The procedure used for the safety simulations closely follows that used for the first time for the SPEAR3 safety simulations [5] and then adopted by other light sources [7, 9]. In this, only a small section of the storage ring between any given insertion device (ID) straight (or the straight section upstream of the bending in the case of the dipole beamline) and respective front ends is considered, as this greatly reduces the number of magnets to include in the simulations and is independent of the lattice configuration.

## 2. METHOD

### 2.1. Outline of simulation procedure

The ALBA storage ring consists of 16 straight sections separated by 16 arc sections. Each arc section contains two bending magnets and a number of quadrupoles, sextupoles, skew quadrupole and corrector magnets. The light from the IDs and bending magnets is extracted along beam-lines which come off at a tangent to the bending magnets. The extraction point where the tangent light path crosses the electron trajectory is at the entrance of the first bending magnet downstream of the ID and in the case of the dipole beam line, it is at a source point close to the centre of the bending.

A beam-line can be considered to be safe to operate in top up mode if any one of the following equivalent statements can be demonstrated to be true [8]:

- It is not possible for a bunch of electrons travelling *forwards* from an ID straight section to pass beyond a pre-determined 'safe point' in the beamline front end.
- It is not possible for a bunch of electrons travelling *backwards* from the beam-line safe point to pass beyond the ID straight section.
- The trajectories of electrons travelling forwards from an ID straight section do not overlap (in position and angle, i.e. in the phase space coordinates) with those of electrons travelling backwards from the safe point in the beam-line at any intermediate location.

Any one of these statements could be used as the basis for the tracking studies, but it is the third statement that the work described in this report aims to demonstrate is true.

The basic procedure is to track all possible particle trajectories forwards from the start of the ID straight to the beginning of the first bending magnet, and to track all possible trajectories from each beamline back to the start of the same bending magnet. The resulting phase-space distributions can then be compared at this location to see whether they overlap for any realistic error scenario.

Possible fault conditions which can arise in the storage ring include an energy mismatch between the injected beam and storage ring magnet strengths, incorrect setting or failure of a magnet, trajectory errors for the injected electron.

Reasonable limits can be placed on the range of errors to include in the simulations. The full range of possible starting trajectories for the forwards and backwards tracked beams can be fixed purely from geometrical considerations in the magnetic field-free regions of the ID straight section, or the straight section upstream of the dipole beamline, and the beamline front end; limits can be placed on the injected beam energy by considering what range is allowed by the injector power supplies, and boundaries can be placed on the bending field errors by considering what can be tolerated before it is no longer possible to store electrons due to the loss of the closed orbit.

## 2.2. Tracking code description

For the simulations, the Matlab-based tracking code Accelerator Toolbox [10] was selected. The motion of particles at very large amplitudes is considered, in particular in the case of the bending magnets and the fields roll-off of the quadrupoles and sextupoles interfering with the front end beam pipe. The new pass methods developed at Diamond [7, 8] were modified for tracking through the ALBA gradient bending magnets. The field profiles data were generated using a finite element analysis code [11].

The results of 2D particle tracking through an ALBA gradient bending using both new and old linear pass methods are shown in Fig. 1 below.

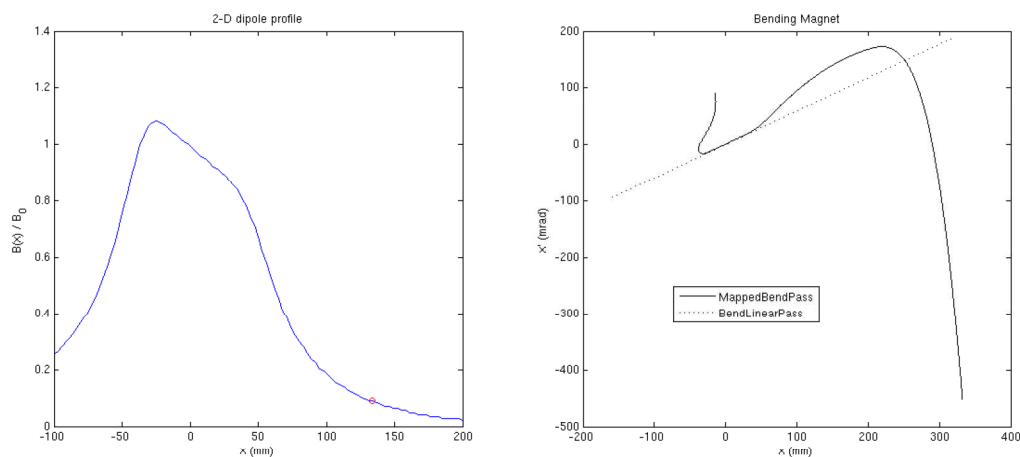


**Figure 1** - Transversal field profile of the ALBA combined function bending (left). The good field region with constant gradient is within -20mm/+30mm, a particle exiting through the front end aperture will experience the roll-off field at  $x = 122$  mm (red circle). Particle trajectories when tracking through a combined function bending magnet (right). The trajectories through the ideal magnet (black dotted line) are shown for comparison with the new pass method including the transverse roll-off (black solid line).

### 2.3. Definition of particle phase spaces

The physical apertures of the ID straight section and beam-line front ends define the region of phase-space to use when generating distributions of particles to track. For the straight sections the limiting apertures are tapers at each end (ID beamlines) or the vacuum chamber aperture (dipole beamline), and for the front ends the limits are given by a fixed aperture at the second fixed mask and the movable mask apertures close to the shield wall. A diagram showing how the phase space limits for the ID straight section are defined is given in Fig. 2.

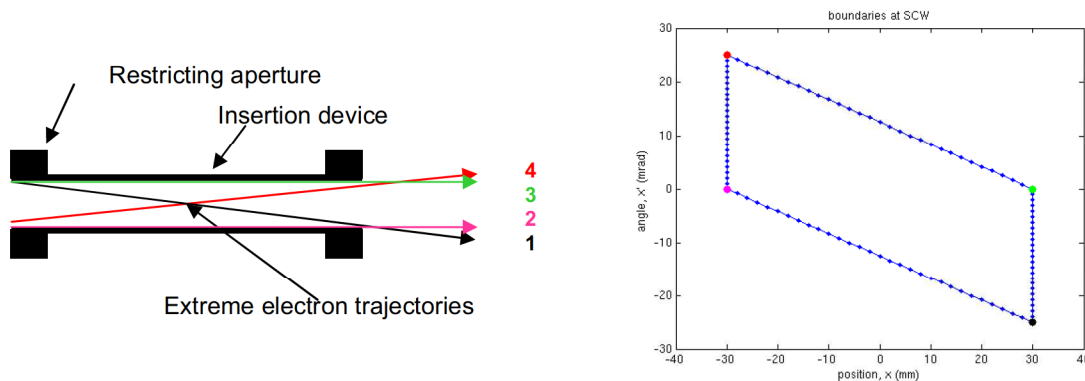


**Figure 2** – Particle trajectories are limited by the tapers at each end of the standard ID straight section (left), the four extreme electron trajectories (colour lines and dots) define the phase space area enclosing all possible electrons trajectories accepted by the straight section. Horizontal phase space boundaries (right, blue line) for particles accepted through the standard ID straight section.

### 2.4. Error Scenarios

#### 2.4.1. Magnet Strength Variations

To retain lattice independence for the results of the tracking studies, all magnet strengths were varied across the full range allowable by the power supplies and no specific setpoint was assumed. Changes to individual magnet strengths were not considered to be an error as such, as they could arise because different operating magnet parameters, power supply failure or simple operator error. Magnet strength variations were therefore scanned in all possible combinations.

Quadrupole magnets have unipolar 200A or 225A power supplies giving a maximum strength of  $2.3 \text{ m}^{-2}$ , and all sextupoles have unipolar 215A power supplies giving a maximum strength of  $34 \text{ m}^{-3}$ . Dipole corrector magnets have bipolar 10A power supplies, giving maximum strengths of  $\pm 1 \text{ mrad}$ .

#### 2.4.2. Aperture Misalignments

The maximum amplitude for all tracked particles is limited by the physical apertures of the vacuum chamber and elements in the beamline front ends. All storage ring apertures used in the simulations are defined in [11, 12] and the front end apertures are described in [12]. To account for any physical misalignments, all apertures have been increased by 1mm in both directions.

#### 2.4.3. Energy Errors

Energy mismatch between the injected and stored beam effectively scales the strength of all intervening magnets. If the injected beam energy is high with respect to the stored beam energy, the magnetic rigidity of the injected beam is high and all magnetic fields appear weaker. Such an energy mismatch could occur due to booster extraction timing errors, booster magnet strength errors or simply by a scaling down of all storage ring magnet strengths.



For the simulations a limit of  $\pm 15\%$  energy error has been placed on the injected beam. This value was chosen as the booster power supplies are rated to give a maximum energy of 3.45 GeV.

### 2.5. Method Demonstration

The basic steps in the tracking are:

1. Determine all possible trajectories for particles passing through the ID straight (forwards tracked beam) and beamline front end (back-tracked beam).
2. Create boundaries in phase-space which enclose all trajectories found in step 1, and use these boundaries to generate the initial phase space coordinates for the particles to track.
3. Track the two distributions to the entrance of the dipole magnet.
4. Compare the resulting distributions to see if they overlap. If an overlap exists, there is a possible route for the injected beam which could lead to a top-up accident.
5. Adjust the strength of the intervening magnets and repeat stages 3 and 4.

Diagrams illustrating the starting conditions for step 3 and corresponding diagram for step 4 are shown in Fig. 3.

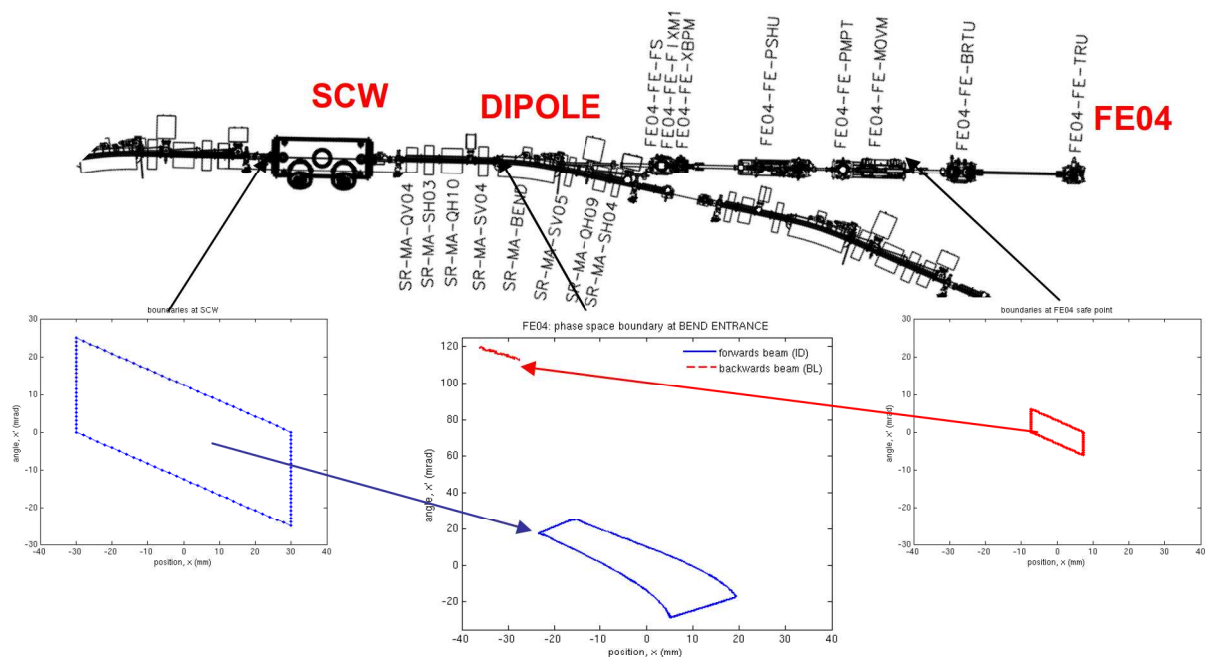


**Figure 3** - Diagram to illustrate the initial and final conditions of the particle tracking. The top drawing shows the section of the storage ring used for the tracking studies in the case of an ID beamline. The lower left hand plot shows the initial phase-space coordinates for the forwards track beam, the lower right hand plot shows the initial coordinates for the back tracked beam, and the lower plot in the centre compares the final two distributions. In this example the two distributions do not overlap, indicating a safe combination of magnet strengths was used.

### 3. ID BEAMLINES (BL04, BL11, BL13, BL22, BL24, BL29)

#### 3.1. Magnet arrangement and apertures

The present six ID beamlines have the same layout: the ID is installed in a medium straight section of the ALBA lattice and the layout of the BL04 front end is shown in Fig. 3 as an example. The electrons exiting the ID travel through two quadrupoles and two sextupoles before entering the bending magnet where the beam line front end is aligned tangent to the entrance point. The front end beam pipe interferes only with one sextupole. The acceptances for all the present insertion device beamlines are shown in Fig. 4, where positions and angles are stated with respect to the stored beam centre line. An aperture boundary enclosing all FE apertures has been defined enlarging by 20% the second mask aperture of FE22: if top-up can be shown to be safe here, then all other beamlines must also be safe. In the subsections 3.2 to 3.5 the effect of each error is scanned separately. In section 3.6 the worst case combining more errors is shown.

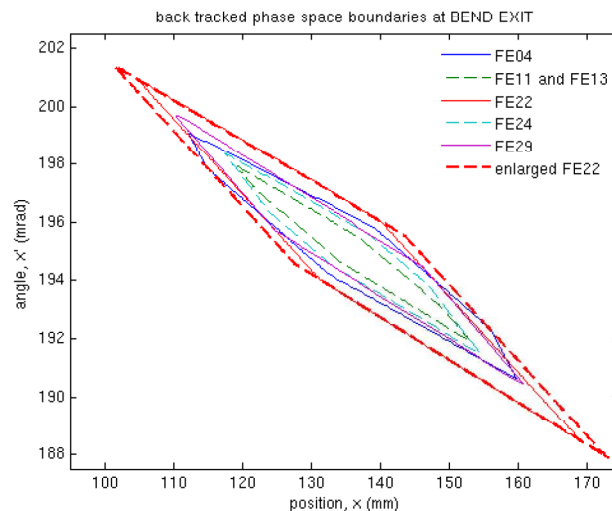


**Figure 4** – Phase space boundaries enclosing all possible trajectories for each one of the ALBA ID beamline front end compared at exit of the bending magnet, where positions and angles are stated with respect to the stored beam centre line. The apertures for individual ID straight sections and BLFEs do not vary significantly in position and angle. Beamline 22 has the largest acceptance. BL22 with the second mask aperture increased by 20% has been defined as the test FE for IDBLs safety simulations: if top-up can be demonstrated to safe for this beamline, all other ID beamlines will be also safe.

#### 3.2. Injected beam energy error

The first error scenario considered was for an energy mismatch between the injected and stored beam energies. Variations in the particle energy will change the trajectory of the particle through the magnetic fields, and an increase in the injected beam energy would have the same effect as decreasing the strength of all magnets in the storage ring.

Figure 5 shows the results of varying the energy by -2.5% to +15%. Values lower than -2.5% are not plotted since particles are scraped by the -36 mm dipole inner aperture. The phase space boundaries are brought closer together with increasing injected beam energy. As can be seen there is a large degree of separation between the phase spaces tracked from the ID straight section and beamline at the entrance of the dipole over this range of energies.

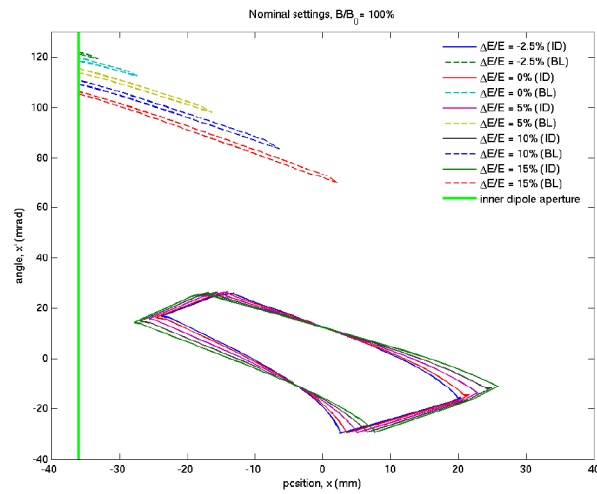


**Figure 5** – Phase space boundaries at the entrance to the bending magnet. Particle energy is varied from the minimum value of -2.5% accepted by front end line aperture (determined by the dipole apertures) and the maximum energy deviation of +15% allowed by the booster bending power supplies.

### 3.3. Single dipole failure

The magnet that has the strongest effect on the particle trajectories is the bending magnet, and clearly if this magnet were switched off the electrons travelling forwards from the ID straight section would follow a straight line trajectory similar to the X-ray beam and pass straight down the beam-line. This is demonstrated in Fig. 6, in which the phase space boundaries for the ID straight section and the beamline when switched off totally overlap.

The phase space boundaries from the ID straight section and beam-line begin to overlap once the bending magnet strength has fallen to 20% of nominal. This situation is not a cause for concern, since simulations have demonstrated it is not possible to store beam with a single dipole at 93% of nominal or below, and the stored beam interlock would inhibit injection.

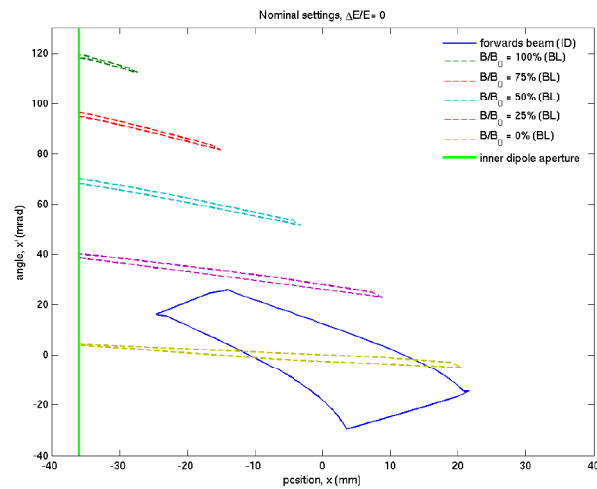


**Figure 6** – Phase space boundaries at the entrance to the bending magnet for different degrees of bending field failure.

### 3.4. Single quadrupole failure

Of the two quadrupoles between the ID straight section and the beamline entrance, the first (defocusing) quadrupole (QV03) brings the phase space boundaries apart. The quadrupole power supplies are capable of delivering 0-200A to the magnets, with the nominal setting for this magnet 164A. The effect of varying this magnet through the full range of possible strengths is shown in Fig. 7, indicating it is when this magnet is switched off that the phase space boundaries are the closest to overlapping. The second (focusing) quadrupole (QH07) main effect is mainly to rotate the phase space boundaries. The quadrupole power supplies are capable of delivering 0-225A to the magnets, with the nominal setting for this magnet 170A. The effect of varying this magnet through the full range of possible strengths is shown in Fig. 7, indicating it is when this magnet is at maximum strength that the phase space boundaries are the closest.

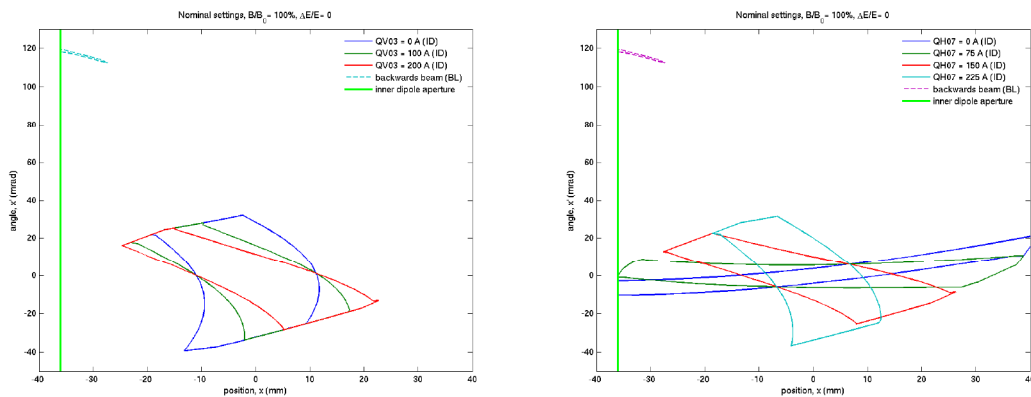


**Figure 7** – Phase space boundaries at the entrance to the bending magnet. QV03 (left) and QH07 (right) have different degrees of failure with field change from zero to maximum allowed by the power supply.

### 3.5. Single sextupole failure

The two sextupoles between the ID straight section and the beamline entrance have very little effect on the phase space boundaries being their effect a small distortion of the distribution. The sextupole power supplies are capable of delivering 0-215A to the magnets, with the nominal setting for these magnets around 160A. The effect of varying these magnets through the full range of possible strengths is shown in Fig. 8, indicating it is when this SH03 is switched off and SV04 is at the maximum strength that the phase space boundaries are brought close together.

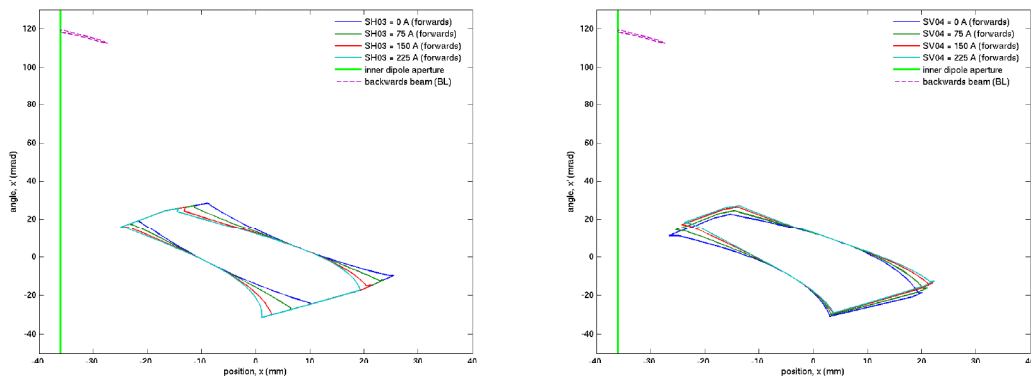


**Figure 8** – Phase space boundaries at the entrance to the bending magnet. SH03 (left) and SV04 (right) have different degrees of failure with field change from zero to maximum allowed by the power supply.



### 3.6. Worst scenario combining events

The procedure outlined in section 2 was carried out varying all magnet strengths in combination across the stated ranges. No error combination where beams overlap was found. The situation where the forwards and backwards tracked beams are the closest to overlapping is shown in Fig. 9. This occurs at injected beam energy offsets of +15%, dipole field at 93% of nominal value, QV03 and SH03 off and QH07 at maximum strength. In this condition the distance between the two phase space boundaries is still larger than 20 mrad.

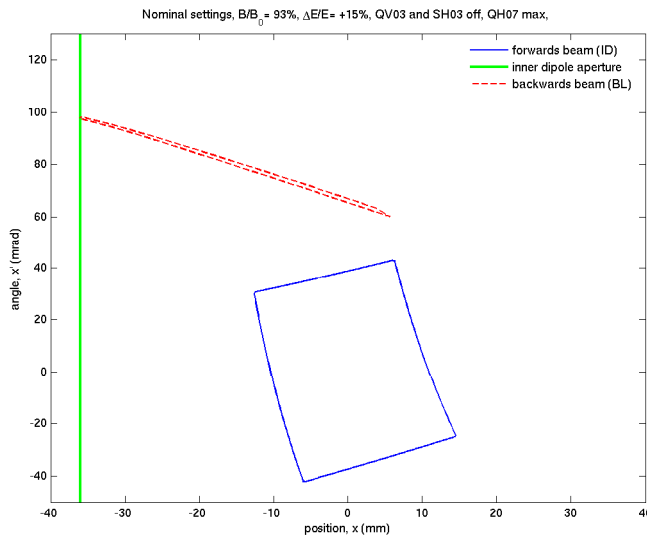


Figure 9 – Phase space boundaries at the entrance to the bending magnet in the situation closest to overlapping.

## 4. DIPOLE BEAMLIN (BL09)

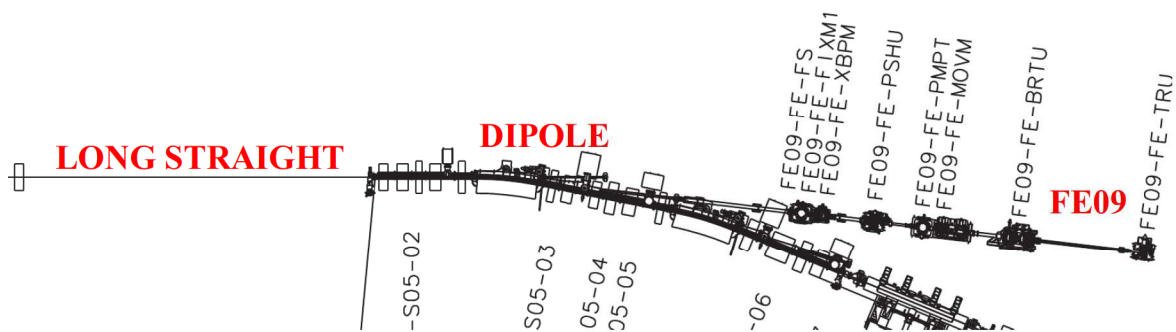
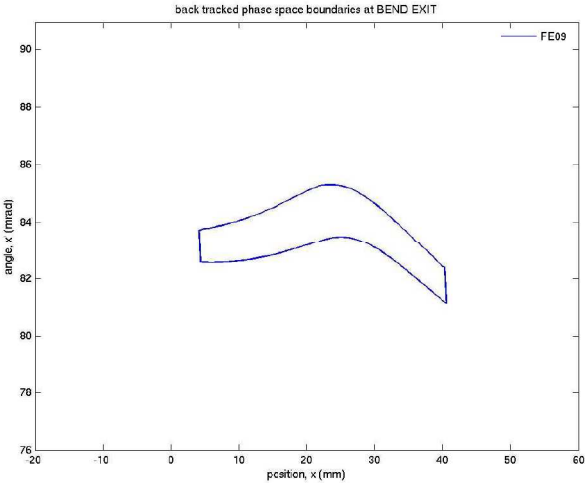


Figure 10 – Layout of the ALBA section used for the tracking studies of the dipole beamline.

### 4.1. Magnet arrangement and apertures

The layout of the dipole beamline is shown in Fig. 10: the radiation produced by the first dipole installed downstream of a long straight section of the ALBA lattice. The electrons exiting the straight travel through three quadrupoles and two sextupoles before entering the bending magnet where the beam line front end is aligned at an angle of  $4.6^\circ$  with respect to the stored beam centre orbit. The front end beam pipe interferes with the roll off field of three sextupoles and three

quadrupoles and the acceptance is shown in Fig. 11, where positions and angles are stated with respect to the stored beam centre line. In the subsections 4.2 to 4.5 the effect of each error is scanned separately. In section 4.6 the worst case combining more errors is shown.



**Figure 11** – Phase space boundaries enclosing all possible trajectories for the ALBA dipole beamline compared at exit of the bending magnet, where positions and angles are stated with respect to the stored beam centre line.

**4.2. Injected beam energy error**

As for the ID beamlines, the first error scenario considered was for an energy mismatch between the injected and stored beam energies. Fig. 12 shows the results of varying the energy by -13% to +15%. Values lower than -13% are not plotted, since particles are scraped by the dipole aperture. The phase space boundaries are brought closer together with increasing injected beam energy. As can be seen there, not only there is a large degree of separation between the phase spaces tracked from the straight section and beamline at the entrance of the dipole over this range of energies, but the backwards tracked beam is always outside of the dipole aperture.

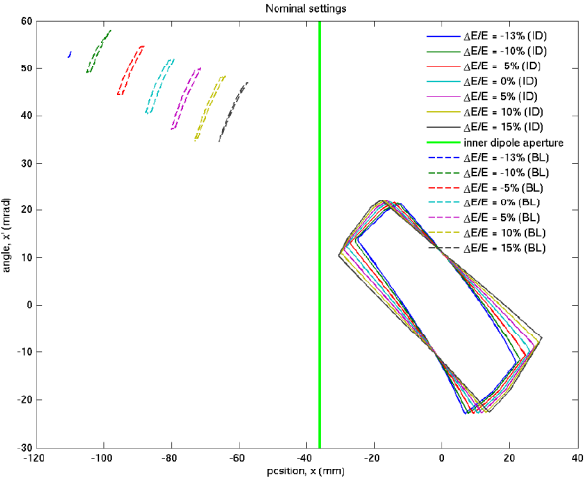


**Figure 12** – Phase space boundaries at the entrance to the bending magnet. Particle energy is varied from the minimum value of -13% and the maximum energy deviation of +15% allowed by the booster bending power supplies. The backtracked beam is always outside of the inner aperture of the dipole vacuum chamber (green line).

### 4.3. Single dipole failure

The magnet that has the strongest effect on the particle trajectories is the bending magnet. For dipoles field higher than 60%, the beamline distribution is always outside of the dipole aperture. In this beamline the if this magnet fall down to 50% the electrons travelling forwards from the ID straight section would follow a straight line trajectory parallel to the X-ray beam at  $4.6^\circ$ , but the position would be 30 mm apart because the alignment does not coincide. This is demonstrated in Fig. 13, in which the phase space boundaries for the straight section and the bending magnet when decreased at 50% have the same angle. This means that at least a second combined error is needed to overlap the two distributions.

In addition to that, as in the ID case, realistic single dipole failures are limited since simulations have demonstrated it is not possible to store beam with a single dipole at 93% of nominal or below, and the stored beam interlock would inhibit injection.

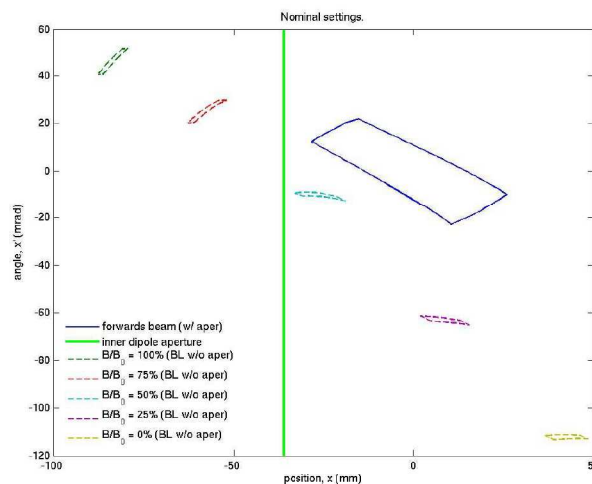


**Figure 13** – Phase space boundaries at the entrance to the bending magnet for different degrees of bending field failure. For  $B > 60\%$  the backtracked beam is always outside of the inner aperture of the dipole vacuum chamber (green line), but even for offsets higher than 40% the two distribution can not overlap.

### 4.4. Single quadrupoles failure

Of the two, the first (defocusing) quadrupole (QV03) brings the phase space boundaries apart. The quadrupole power supplies are capable of delivering 0-200A to the magnets, with the nominal setting for this magnet 164A.

The effect of varying the three quadrupoles between the straight section and the beamline entrance through the full range of possible strengths is shown in Fig. 14-left, indicating it is when this magnet are around the nominal strengths (150A circa) that the forwards tracked phase space distribution is brought the closest to overlapping. But it is in the beamline distribution that the tracking studies were concentrated in order to look for possible combined errors that bring the particles inside beyond the inner dipole aperture represented by the green line in the phase space plots. In facts plots in Fig. 14-right shows that roll off quadrupole fields have very little effect.

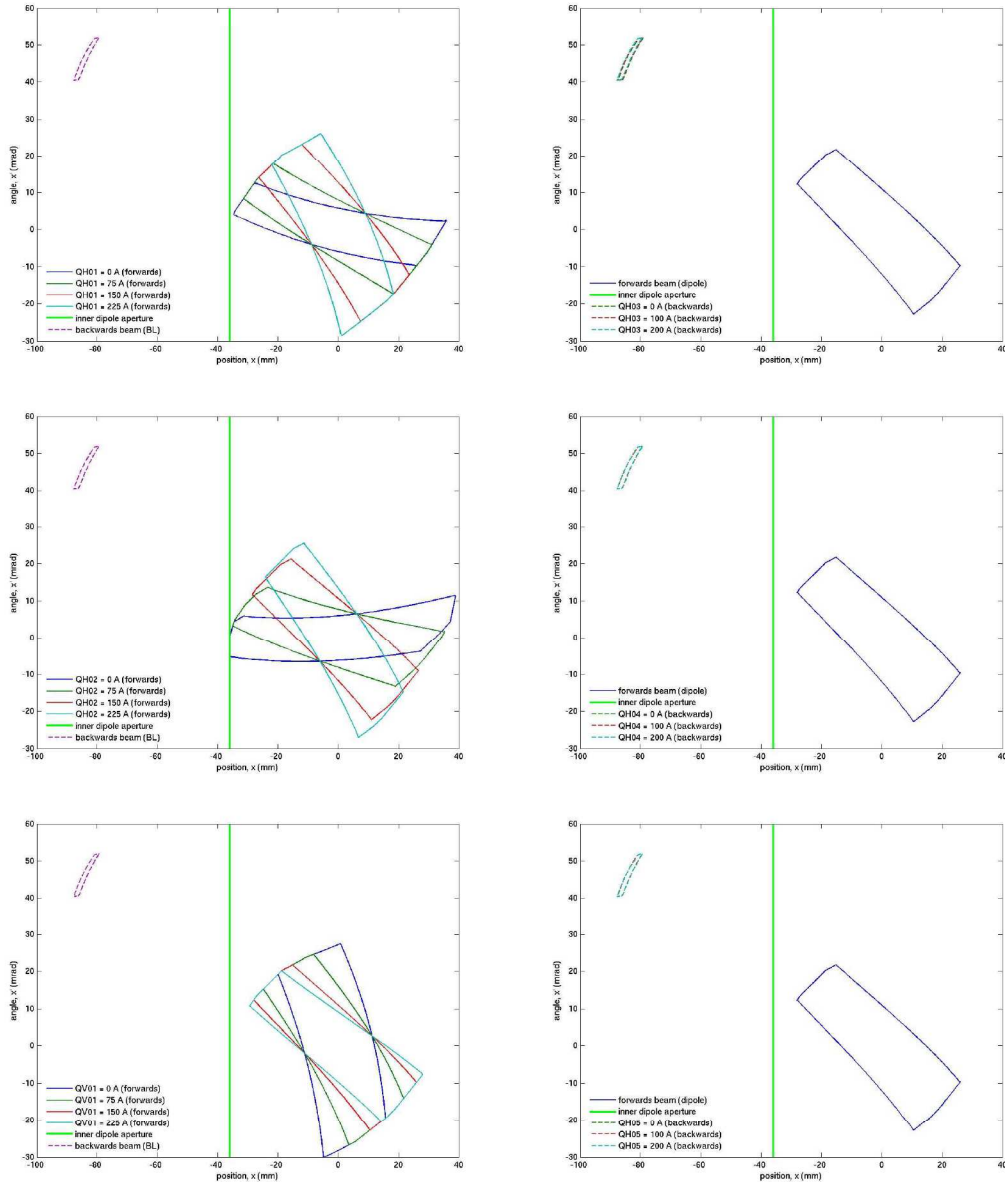


**Figure 14** – Phase space boundaries at the entrance to the bending magnet, for different degrees of QH01, QH02 and QV01 (left) and QH03, QH04, QH05 (right) field failure. The plots at the left show that the effect of the quadrupole roll off field is negligible, the backtracked beam is always outside of the inner aperture of the dipole vacuum chamber (green line) and field failure.

#### 4.5. Single sextupole failure

The two sextupoles between the straight section and the beamline entrance have very little effect on the phase space boundaries being their effect a small distortion of the distribution. The sextupole power supplies are capable of delivering 0-215A to the magnets, with the nominal setting for these magnets around 160A. The effect of varying these magnets through the full range of possible strengths is shown in Fig. 8, indicating it is when this SH01 is switched off and SV01 is at the maximum strength that the phase space boundaries are brought close together.

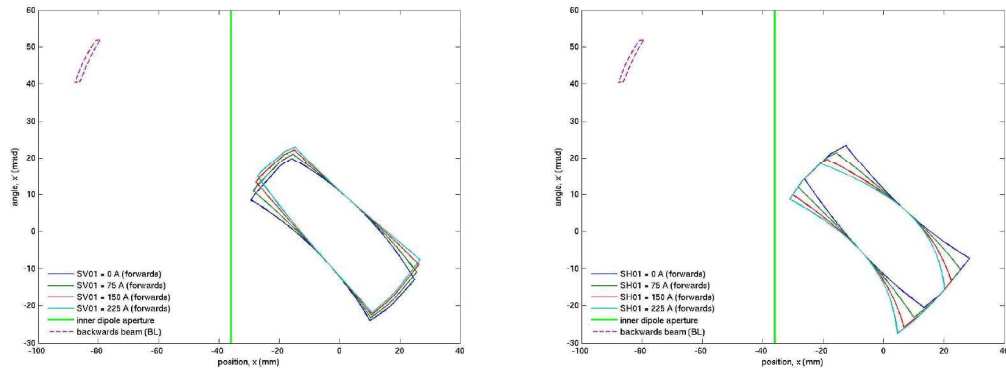


**Figure 15** – Phase space boundaries at the entrance to the bending magnet, for different degrees of SV01 and SH01 field failure.

The three sextupole roll-off field in the beamline beam pipe have some deflecting effect on the phase space distribution. The effect of varying these magnets through the full range of possible strengths is shown in Fig. 16, indicating it is when this SV02 and SV03 are switched off and SH02 is at the maximum strength that the phase space boundary is deflected towards inside the dipole aperture.

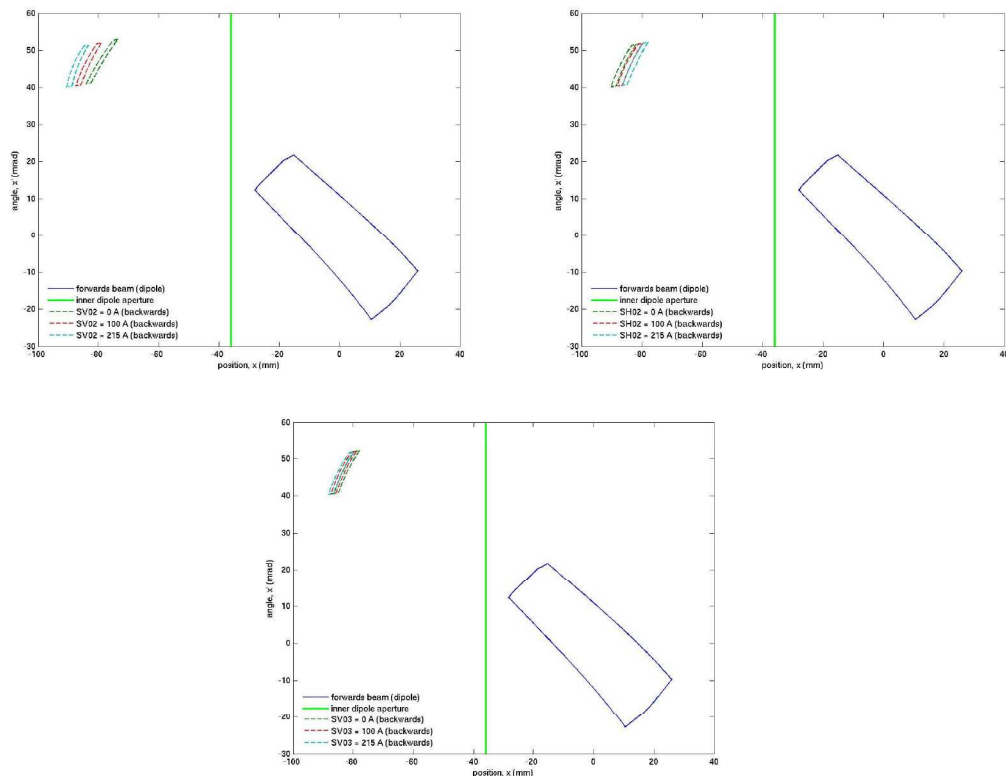


**Figure 16** – Phase space boundaries at the entrance to the bending magnet, for different degrees of SV02, SH02, SV03 field failure.



#### 4.6. Worst scenario combining events

The procedure outlined in section 2 was carried out varying all magnet strengths in combination across the stated ranges. Not only no error combination where beams overlap was found, but no situation where the backwards tracked beam is not lost through the dipole vacuum chamber was found. The situation where the forwards and backwards tracked beams are brought to the closest distance is shown in Fig. 17. This occurs at injected beam energy offsets of +15%, dipole field at 93% of nominal value, SV02 and SV03 off, and SH02 at maximum strength. In this condition the distance between the two phase space boundaries is still larger than 15 mrad and 15 mm.

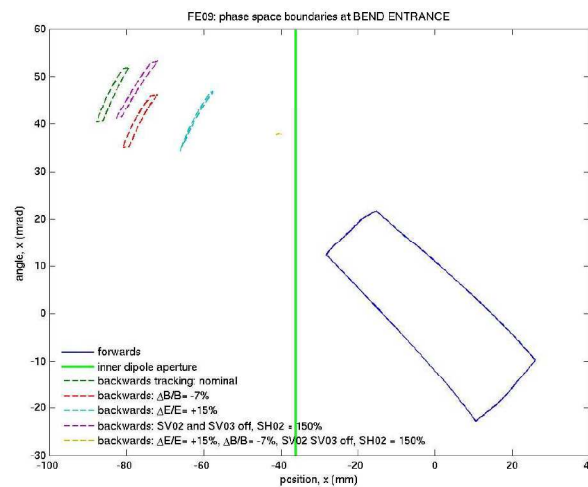


Figure 17 – Phase space boundaries at the entrance to the bending magnet in the situation of minimum distance.

## 5. DISCUSSION

The primary aim of the work described in this report was to determine if it is possible for a stray beam of injected electrons to exit through an open beamline shutter under any fault conditions, with the secondary aim of identifying effective interlocks which would prevent such a situation from occurring, should such a scenario be found.

At ALBA it has been demonstrated that neither a single error nor more combined events would be sufficient to lead to a top-up accident, even in the absence of interlocks. The one exception to this statement is for a single dipole to be below 20% of nominal strength with all other dipoles at full field. For this last case the stored beam interlock already guarantee that a single dipole field can not be below 7% of nominal value.

The method chosen to investigate the possibility of a top-up accident occurring has proven to be an effective one. Monitoring the behaviour of the phase-space boundaries gives a good intuitive feel for the consequences of a particular type of magnet failure and as such it has proved unnecessary to simulate every single setting for each magnet of the storage ring.

### Acknowledgements

Many thanks to I. Martin, for advising and providing the sample of his new AT pass methods, they have been the starting point of this study. M. Pont, J. Marcos and J. Campmany are gratefully acknowledged for providing the magnet, aperture and insertion device data used throughout this study. Conversations with M. Munoz and Z. Marti have been also very useful.